EFFECT OF TENSILE FATIGUE LOAD ON CAPACITANCE OF STRUCTURED CAPACITORS MADE OF CFRP

K. Miura[1]*, K. Obunai[2], K. Okubo[2]

[1] *Graduate School of Science and Engineering, Doshisha University, Kyotanabe, Kyoto, Japan*
[2] *Department of Mechanical Engineering, Doshisha University, Kyotanabe, Kyoto, Japan*
** Corresponding Author E-mail:ctwh0548@mail4.doshisha.ac.jp*

Keywords: Laser Induced Graphene, supercapacitor, CFRP

Abstract

The purpose of this study is to investigate the mechanical and electrical characteristics of structured supercapacitor fabricated by combining CFRP and planer type supercapacitor under static and cyclic tensile load. The planer type supercapacitor was made from thin polyimide film and solid electrolyte. The electrode of supercapacitor was fabricated by irradiating the UV laser to polyimide film to synthesize laser induced graphene. The solid electrolyte was synthesized from H_3PO_4 and PVA, and it was applicating on electrode by casting method. To fabricate the structured supercapacitor, the 3K plain woven carbon cloth was used as reinforcement, and thermoset epoxy resin was used as matrix. The stack of 4 layer of carbon clothes and the supercapacitor was prepared to impregnate the epoxy resin. The static mechanical characteristics and electric characteristics of structured supercapacitor was investigated by uniaxial tensile test. The changes in capacitance and electric resistance under cyclic tensile fatigue load was also measured. Static tensile test results showed that, as the tensile strain of structured supercapacitor increased, the capacitance was decreased, while electrical resistance of electrode increased. The fatigue test results also indicated that the capacitance of the supercapacitor exhibited an exponential decrease with an increase in the number of cycles. Additionally, it was observed that the degree of capacitance decrement increased with an increase in the maximum stress level.

1. Introduction

Recently, supercapacitors (SCs) have been attracting attention as an alternative to batteries for energy storage applications [1]. This is due to their long-life span and ability to rapidly charge and discharge [2]. Previous studies have proposed a novel fabrication process for electric double-layer SCs in which the electrodes are made from laser induced graphene (LIG) by irradiating a UV laser on Polyimide (PI) films [3-5]. The major advantages of these new types of SCs (hereafter referred to as planar-SCs) are their thin profile, flexibility and long lifespan through thousands of cycles [6]. However, due to their thin and flexible nature, planar-SCs cannot bear the external load on their own. A previous study conducted by the authors demonstrated that by inserting planar-SCs into the inter-layer of carbon fiber reinforced plastics

(CFRP) and fabricating structured SCs, can significantly enhance the load bearing capabilities compared to that of planar-SCs alone [7].

The purpose of this study is to investigate the electrical characteristics of structured SCs under static and fatigue load. The capacitance change of structured planar-SCs was measured using the cyclic voltammetry (CV) method. Additionally, the resistance change of the LIG electrode was also measured.

2. Experiment methods

2.1 Materials

A 125 μm thickness of PI film (Kapton, Toray-Dupont) was used as substrates for the planar-SCs. LIG was synthesized on the surface of PI film using a 2-axis laser engraver (ATOMSTACK A5 10W) with a laser wavelength of 405nm. The semi-solid electrolyte for planar-SCs was fabricated from PVA (average degree of polymerization 1500~1800, Fuji Film) and H_3PO_4 (85%, Fuji Film).

PAN-based plain woven carbon fiber cloth (TR3110M, Mitsubishi Chemical) was used as a reinforcement for CFRP. Epoxy resin (jER828, Mitsubishi Chemical) and curing agent (jER Cure 113, Mitsubishi Chemical) were used for matrix of CFRP.

2.2 Preparation of planer-SCs

Figure1 show geometries of electrode used in this study. An interdigitated electrode was fabricated on the 40×110 mm² of PI film. The width and length of each electrode were 1.5 and 13 mm, respectively, and the spacing between the electrodes was 0.5 mm. Current collectors were provided above and below the interdigitated electrodes. The power and scanning speed of UV laser were controlled to be 300 mW and 600 mm/min, respectively, and the electrode shape was engraved by raster scan. After engraving the electrode shape, PI film was rinsed with acetone to remove the dust. A 70 μm thick Cu tapes (3M CU-35C) were attached to the current collectors as a tab lead. Here, the electrical resistance of the LIG electrode was measured between points A and A' as illustrated in Figure 1, while the capacitance of planer-SCs was measured between points B and B'. The H_3PO_4/PVA semi-solid electrolyte was prepared by adding 1 g of PVA and 1.3 mL of H_3PO_4 to 18.7 mL of purified water and stirring it at 95°C for 15 minutes. The H_3PO_4/PVA electrolyte was dropped onto the electrode as illustrated blue color and solidified in a desiccator at room temperature.

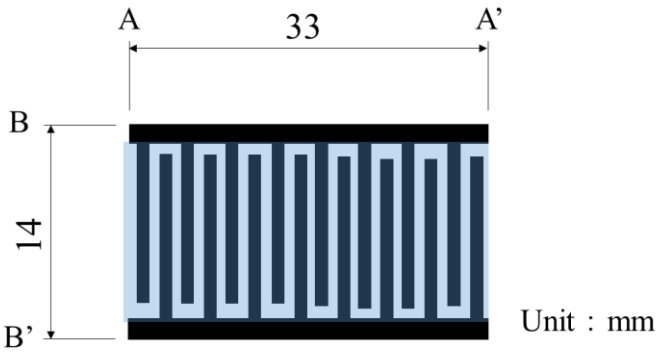

Figure 1. Schematic illustration of LIG electrode.

2.3 Preparation of structured SCs

Figure2 shows the schematic illustration of structured SCs. The hand layup method was employed to fabricate the CFRP. The laminate configuration of the CFRP was $[0\text{-}90]_4$ and the

planar-SCs was inserted between the second and third layers of plain-woven carbon fiber cloth. The prepared resin was impregnated to the stacks by roller. After lamination, the matrix resin was cured by heat press machine under 2.0MPa of pressure at 60 ℃ for 3 hours. To avoid the slippage during testing, 1.0 mm thickness of aluminum tabs were adhered to the structured SCs. The longitudinal direction of planer-SCs and CFRP were aligned as illustrated in Figure2.

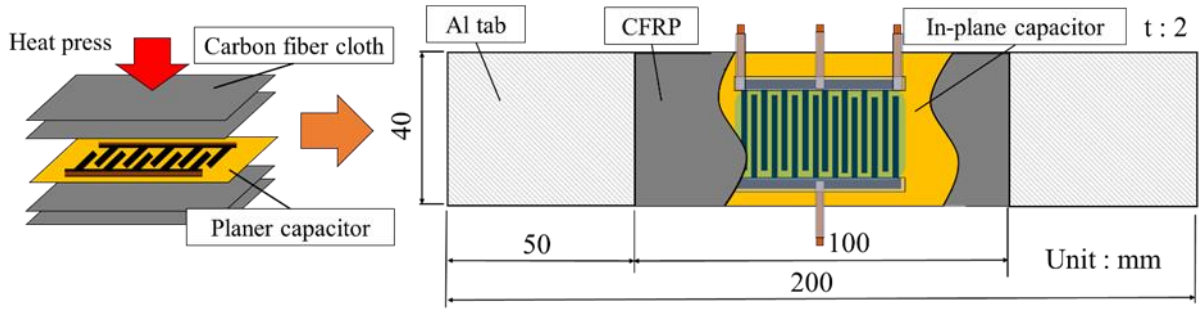

Figure 2. Fabrication processes and geometries of structured capacitor.

2.4 Cyclic voltammetry test

The capacitance of the structured SCs was measured by cyclic voltammetry (CV) technique. The electrode potential of SCs was ramped to limit potential at specific scan rate. Then, the potential of working electrode was reduced to initial potential at specific scan rate. During potential variation, the current of working electrode was measured as a function of its potential. By using the obtained current and potential of working electrode, CV diagram was plotted to evaluate the capacitance by measuring the area enclosed by CV diagram. Following equation was used to calculate normalized capacitance of structured capacitor.

$$C_A = \frac{1}{2 \times A_C \times v \times (V_f - V_i)} \int_{V_i}^{V_f} I(V) dV \quad (1)$$

Here, A_C, v, V_i, V_f, and $I(V)$ denote the nominal area of the SCs, potential scan rate, initial potential, limit potential, and current at different potential, respectively. In this study, scan rate and limit potential for CV measurements were set to 10 mV/s and 500 mV, respectively. The blue colored area illustrated in Fig. 1 (1.4 x 3.3 cm²) was used for the nominal area of the SCs (A_C).

2.5 Static tensile test

The capacitance changes of structured SCs and electrical resistance changes of LIG electrode were measured under static tensile load. The static tensile load was applied to the structured SCs by using a universal testing machine (Autograph AG-I, Shimadzu). The tensile strain of structured SCs was measured by using a strain gauge attached to the surface of specimen. The capacitance changes of structured SCs and electrical resistance change of LIG electrode were measured by using a Potentiostat/Galvanostat (SDPS-511U, syrinx) and digital multimeter (R6871, Advantest).

2.6 Tensile-tensile fatigue test

The capacitance changes of structured SCs and electrical resistance changes of LIG electrode were measured under cyclic tensile load. The 4 Hz of sinusoidal tensile load was applied to the structured SCs by using electro-hydraulic servo fatigue testing machine (Servo Pulsar, Shimadzu). At every 1×10^n cycle (n=2,3,4,5), the test was pended and unloaded the

specimen for measuring the capacitance and electrical resistance. The stress ratio R was set to 0.1. The maximum cyclic stress σ_{max} was set to 60 and 80% of average static tensile strength σ_T of structured SCs. In this study, the fatigue test was terminated when the number of cycles reached 10^5 cycles.

Results and Discussion

3.1 Capacitance and electrode resistance changes under static tensile loading

Figure 3 shows the typical stress-strain diagram of structured SCs. The figure also indicated changes in resistance of electrode and capacitance of embedded planer-SCs. Test results showed that, as the tensile strain of structured SCs increased, the capacitance of embedded planer-SCs was decreased, while electrical resistance of LIG electrode increased. These results can be explained as follows; Due to the deformation of the embedded planar-SCs, the LIG electrode on the surface of the planar-SCs undergoes deformation, leading to an increased electrical resistance. Consequently, according to Ohm's law, the electrical current flowing in the planar-SCs decreases. As a results, the capacitance of planer-SCs calculated by equation (1) was decreased. These results also suggest that the changes in electrical resistance and capacitance of structured SCs can be useful parameters for predicting the deformation of the structured SCs under static load.

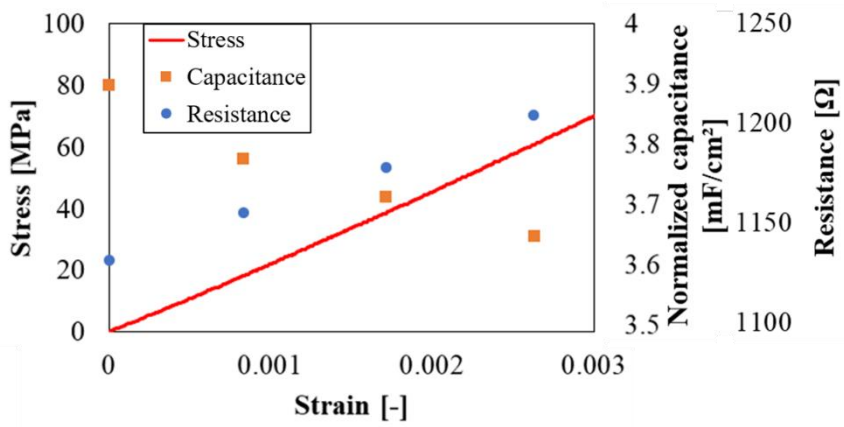

Figure 3. Stress-strain diagram and changes in resistance of electrode and capacitance of planer-SCs.

3.2 Effect of tensile fatigue load on capacitance

Figure4 and 5 show the typical CV diagrams of structured SCs obtained during the fatigue test at 60 and 80% of the applied maximum stress level relative to the tensile strength, respectively. The test results revealed that the area enclosed by the CV diagram decreased with an increase in the number of cycles. Additionally, it was observed that the decrement of the area was greater as the applied maximum stress level increased. Figure6 also shows the changes in capacitance of the structured SCs as a function of the number of cycles. The test results indicated that the capacitance of the structured SCs exhibited an exponential decrease with an increase in the number of cycles. Additionally, it was observed that the degree of capacitance decrement increased with an increase in the maximum stress level. Figure 7 shows the relationship between the capacitance change and the resistance change of the structured SCs during the fatigue test. The test results confirmed an almost negative proportional relationship between the capacitance change and the resistance change, even when different maximum stress levels were applied. These results not only indicate that the capacitance change of structured SCs can be explained by the corresponding change in resistance as previously discussed, even

when subjected to fatigue load, but also suggest that the residual deformation of structured SCs can be effectively measured through the capacitance change.

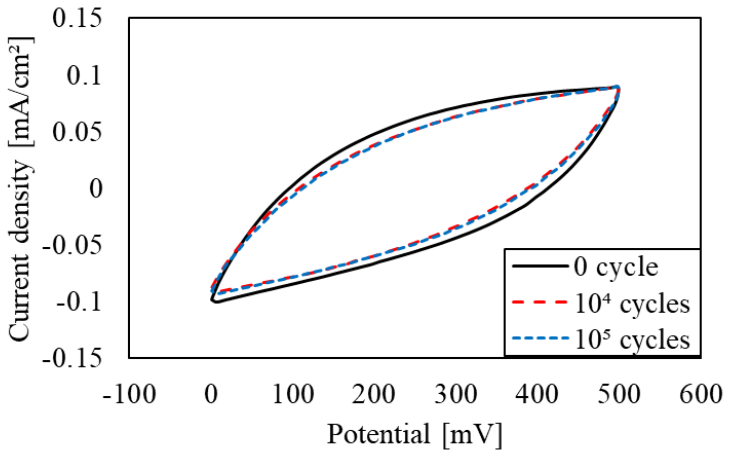

Figure 4. CV diagrams of structured SCs during fatigue test at the maximum cyclic stress set to 60% of average static tensile strength.

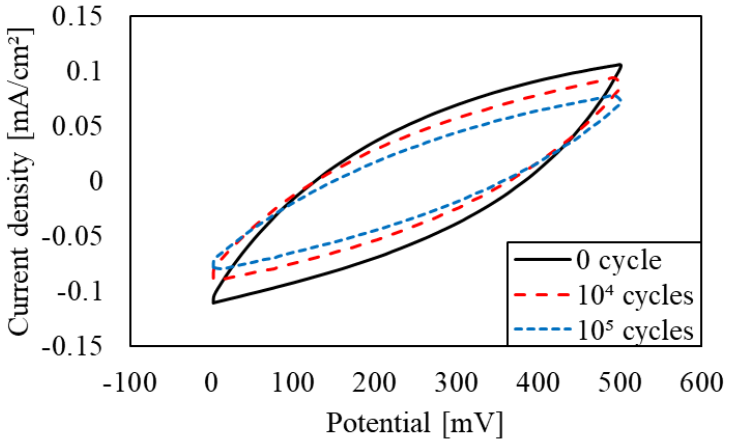

Figure 5. CV diagrams of structured SCs during fatigue test at the maximum cyclic stress set to 80% of average static tensile strength.

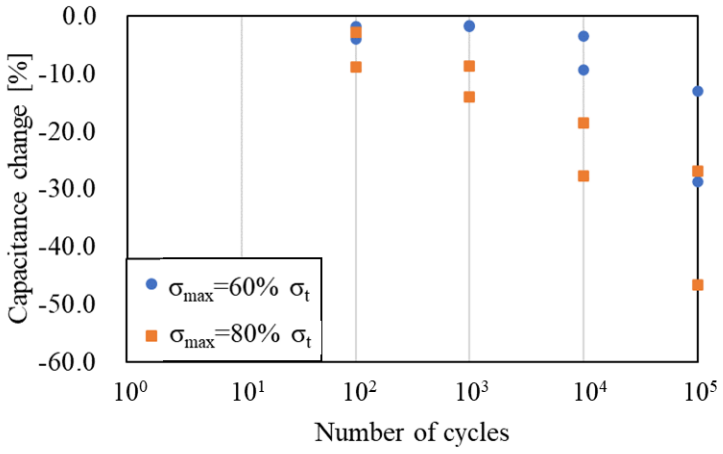

Figure 6. Changes of capacitance of structured capacitor with respect to applied number of cycles.

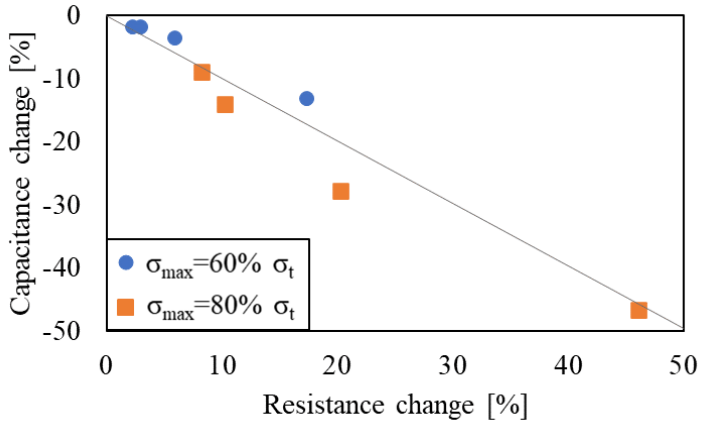

Figure 7. Relationship between the capacitance changes and the resistance changes of the structured SCs during the fatigue test.

3.3 Residual tensile strength of the structured SCs

Figure8 shows the relationship between the residual tensile strength of the structured SCs after 10^5 cycles of fatigue test and the corresponding degree of capacitance decrement. The test results show that the residual tensile strength of the structured SCs was decreased with an increase in the maximum stress level during fatigue test. Additionally, the test results revealed that the residual tensile strength of the structured SCs decreased with an increase in the degree of capacitance decrement. These results suggest that the capacitance change of structured SCs can be an effective parameter for evaluating the residual tensile strength of structured SCs during fatigue test.

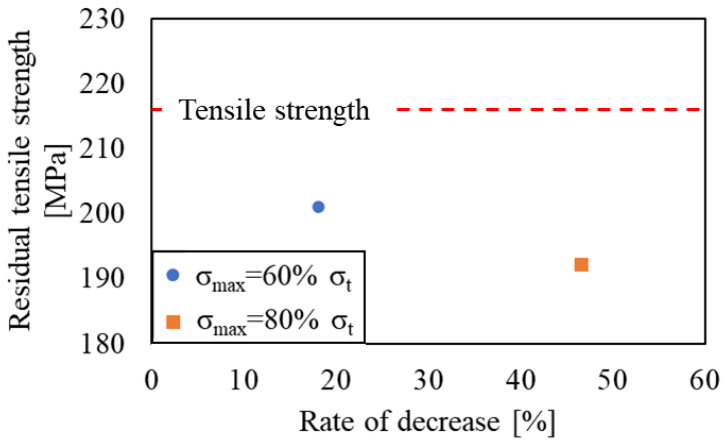

Figure 8. Relationship between the residual tensile strength after fatigue test of the structured SCs and the rate of capacitance decrease.

Conclusions

(1) When the tensile strain of structured SCs increased, the capacitance of embedded planer supercapacitor was decreased, while electrical resistance of laser induced graphene electrode increased.

(2) During fatigue test, the capacitance of the structured SCs exhibited an exponential decrease with an increase in the number of cycles.

(3) The changes in electrical resistance and capacitance of structured supercapacitor can be useful parameters not only for predicting the deformation of the structured SCs under static load, but also predict the residual tensile strength under fatigue load.

Acknowledgment

This work was financially supported by a research project on "Research and Development Center for Advanced Composite Materials" of Doshisha University.

References

[1] Chenguang Liu, Zhenning Yu, David Neff, Aruna Zhamu, and Bor Z. Jang,' Graphene-Based Supercapacitor with an Ultrahigh Energy Density', Nano Lett, 10, pp.4863-4868 (2010)

[2] Nitin Muralidharan, EtiTeblum, Andrew S.Westover, Deanna Schauben, AnatItzhak, Merav Muallem, Gilbert D. Nessim & Cary L. Pint, " Carbon Nanotube Reinforced Structural Composite Supercapacitor", SCIENTIFIC REPORTS, Article number 17662, (2018)

[3] Jinguang Cai , Chao Lv , Akira Watanabe "Cost-effective fabrication of high-performance flexible all-solid-state carbon micro-supercapacitors by blue-violet laser direct writing and further surface treatment" , Journal of Materials Chemistry A, Vol.4 ,pp.1671-1679 , (2016)

[4] Kévin Brousse, Sébastien Pinaud, Son Nguyen, Pier-Francesco Fazzini, Raghda Makarem, Claudie Josse, Yohann Thimont, Bruno Chaudret, Pierre-Louis Taberna, Marc Respaud, and Patrice Simon "Facile and Scalable Preparation of Ruthenium Oxide-Based Flexible Micro-Supercapacitors", Advanced energy materials, Vol.10. 1903136, (2020)

[5] Shutong Wang, Yongchao Yu, RuozhouLi,Guoying Feng. Zili Wu, Giuseppe Compagnini, Antonino Gulino, Zhili Feng, Anming Hu, "High-performance stacked in-plane supercapacitors and supercapacitor array fabricated by femtosecond laser 3D direct writing on polyimide sheets" Electrochimica Acta, Electrochimica Acta, Vol.241, pp.153-161, (2017)

[6] Engy Ghoniem, Shinsuke Mori, Ahmed Abdel-Moniem, 'Low-cost flexible supercapacitors based on laser reduced graphene oxide supported on polyethylene terephthalate substrate', Journal of Power Sources, Vol.324, pp.272-281, (2016)

[7] Kanta Miura, Kiyotaka Obunai, Kazuya Okubo, 'Effect of mechanical load on capacitance of structured capacitor made of CFRP', Proceedings of the 72nd JSMS Annual Meeting, 526, (2023) (in Japanese)